NeuroImage 208 (2020) 116440

Contents lists available at ScienceDirect

NeuroImage

journal homepage: www.elsevier.com/locate/neuroimage

Linking the impact of aging on visual short-term memory capacity with changes in the structural connectivity of posterior thalamus to occipital cortices

Aurore Menegaux [a,b,c,d,*], Felix J.B. Bäuerlein [e], Aliki Vania [a], Natan Napiorkowski [a,b,f], Julia Neitzel [g,h], Adriana L. Ruiz-Rizzo [a], Hermann J. Müller [a,b], Christian Sorg [c,d,i], Kathrin Finke [a,b,f]

[a] Department of Psychology, General and Experimental Psychology, Ludwig-Maximilians-Universität München, Leopoldstrasse 13, 80802, Munich, Germany
[b] Graduate School of Systemic Neurosciences GSN, Ludwig-Maximilians-Universität, Großhaderner Strasse 2, 82152, Planegg, Germany
[c] Department of Neuroradiology, Klinikum Rechts der Isar, Technische Universität München, Ismaninger Strasse 22, 81675, Munich, Germany
[d] TUM-Neuroimaging Center, Technische Universität München, Ismaninger Strasse 22, 81675, Munich, Germany
[e] Department of Molecular Structural Biology, Max Planck Institute of Biochemistry, 82152, Martinsried, Germany
[f] Hans-Berger Department of Neurology, Jena University Hospital, Erlanger Allee 101, 07747, Jena, Germany
[g] Institute of Stroke and Dementia Research, Klinikum der Universität München, Feodor-Lynen-Straße 17, 81377, Munich, Germany
[h] German Center for Neurodegenerative Diseases (DZNE) e.V. Munich, Feodor-Lynen-Straße 17, 81377, Munich, Germany
[i] Department of Psychiatry, Klinikum Rechts der Isar, Technische Universität München, Ismaninger Strasse 22, 81675, Munich, Germany

ARTICLE INFO

Keywords:
Aging
Diffusion tensor imaging
Neural theory of visual attention
Posterior thalamus
Visual short-term memory capacity

ABSTRACT

Aging impacts both visual short-term memory (vSTM) capacity and thalamo-cortical connectivity. According to the Neural Theory of Visual Attention, vSTM depends on the structural connectivity between posterior thalamus and visual occipital cortices (PT-OC). We tested whether aging modifies the association between vSTM capacity and PT-OC structural connectivity. To do so, 66 individuals aged 20–77 years were assessed by diffusion-weighted imaging used for probabilistic tractography and performed a psychophysical whole-report task of briefly presented letter arrays, from which vSTM capacity estimates were derived. We found reduced vSTM capacity, and aberrant PT-OC connection probability in aging. Critically, age modified the relationship between vSTM capacity and PT-OC connection probability: in younger adults, vSTM capacity was negatively correlated with PT-OC connection probability while in older adults, this association was positive. Furthermore, age modified the microstructure of PT-OC tracts suggesting that the inversion of the association between PT-OC connection probability and vSTM capacity with aging might reflect age-related changes in white-matter properties. Accordingly, our results demonstrate that age-related differences in vSTM capacity links with the microstructure and connectivity of PT-OC tracts.

1. Introduction

Our visual system is constantly confronted with more stimuli than it can process and represent. Indeed, the number of objects that can be simultaneously perceived and consciously stored in visual short-term memory (VSTM) is limited (Sperling, 1960; Cowan, 2001). vSTM is the active maintenance of visual representations for further ongoing mental operations as well as voluntary and task-appropriate actions (e.g Luck and Vogel, 2013). Many studies have shown that the individual vSTM capacity accounts for substantial amount of variance in performance in diverse neuropsychological tasks and intellectual capabilities (Cowan, 2010; Fukuda et al., 2010; Johnson et al., 2013; Luck and Vogel, 2013;

Abbreviations: vSTM, visual short-term memory; TVA, theory of visual attention; NTVA, neural theory of visual attention; FA, fractional anisotropy; MD, mean diffusivity; RD, radial diffusivity; AD, axial diffusivity; PT-OC, posterior thalamus – occipital cortex; ROI, region of interest; IQ, intelligence quotient; WM, white matter; GM, grey matter; CSF, cerebrospinal fluid.

* Corresponding author. Department of Psychology, General and Experimental Psychology, Ludwig-Maximilians-Universität München, Leopoldstrasse 13, 80802, Munich, Germany.
E-mail address: aurore.menegaux@tum.de (A. Menegaux).

https://doi.org/10.1016/j.neuroimage.2019.116440
Received 12 October 2019; Received in revised form 25 November 2019; Accepted 3 December 2019
Available online 11 December 2019

Nyberg et al., 2012). Therefore, vSTM capacity is regarded as a major determinant of the maintenance of cognitive capabilities and functional independence at old age (Cowan, 2010; Salthouse, 1994). While it has been suggested that age-related decline in vSTM might result from problems in associative binding of different item characteristics in an episodic trace (e.g., Chen and Naveh-Benjamin, 2012; Naveh-Benjamin, 2000), or from a decline in the precision of vSTM representations (Noack et al., 2012; Peich et al., 2013; Pertzov et al., 2015), there are also several studies showing that the number of items stored itself is reduced (Verhaegen et al., 1993; Gazzaley et al., 2005; Jost et al., 2011; Sander et al., 2011 McAvinue et al., 2012). Some of these studies used the Theory of Visual Attention (TVA) framework (Bundesen, 1990), which conceives visual processing as a race among objects of the visual field to be represented in vSTM, Based on modelling performance in a psychophysical whole-report task, parametric estimates of vSTM capacity (parameter *K*), are retrieved. These estimates of *K* are typically around 3 to 4 items in healthy young participants (e.g. Finke et al., 2005), which is in line with typical estimates of vSTM capacity obtained using alternative paradigms (Cowan et al., 2001; Luck and Vogel, 1997; Vogel and Mechizawa, 2004). A significant advantage of the TVA-based methodology is that vSTM capacity estimation is controlled for potential influences of increased visual threshold and/or visual processing speed (Salthouse, 1996) in aging individuals by separate and independent estimations of these parameters (e.g Habekost and Starrfelt, 2009). Importantly, as stated in the information degradation hypothesis (Monge and Madden, 2016; Schneider and Pichora-Fuller, 2000) without such control for degraded perceptual input signals due to age-related neurobiological processes, perceptual processing deficits might affect the measurement of cognitive functions, such as vSTM capacity. For example, McAvinue and colleagues have reported that vSTM capacity, or parameter *K* in TVA, declined linearly with increasing age. The significant reduction of this parameter has since been replicated in various studies (Wiegand et al., 2014a, 2014b, 2018).

The age-related decline of visual cognitive functions has been suggested to result from neural challenges in form of, for example, cortical thinning and white matter integrity loss, particularly in posterior areas of the brain, which might be compensated to some degree by additional recruitment of frontal areas, as suggested in the "Posterior-Anterior Shift in Aging" model (PASA model; Davis et al., 2008) or more bilateral brain areas, as suggested in the Scaffolding Theory of Aging and Cognition (STAC; Park and Reuter-Lorenz, 2009; Reuter-Lorenz and Park, 2014). Based on the cognitive specificity of the distinct TVA parameters and on the neural interpretation of TVA at both the brain's cellular and systems level in the neural theory of visual attention (NTVA; Bundesen et al., 2005), a more specific, hypothesis-driven examination of the underlying neural mechanisms of age effects particularly on vSTM storage capacity is possible.

NTVA proposes that 'visual' brain regions such as occipital cortices, thalami as well as white matter (WM) tracts connecting those regions are of particular relevance for vSTM capacity in healthy individuals. According to TVA, visual processing involves a race among objects to be represented in vSTM and thus available for conscious report. The winning objects are assumed to be categorized in a vSTM map of locations positioned in the posterior thalamus and particularly in the thalamic reticular nucleus. In line with Hebb (1949) for example, the NTVA assumes that the activity of the neurons representing the winner objects in visual cortices is sustained and reactivated by a feedback loop gated by the thalamic reticular nucleus (Bundesen et al., 2005). Given the critical role assigned to posterior thalamus and visual cortices in NTVA, the structural connectivity between those two regions would be decisive for vSTM capacity (Bundesen et al., 2005) and any alterations in such connections would affect vSTM capacity. TVA-based evidence for a critical role of WM connections in vSTM storage comes from a study by Habekost and Rostrup (2007), who found deficits in vSTM capacity in patients with lesions to posterior tracts. First empirical support for the suggested relevance of posterior thalamic tracts comes from two studies by Menegaux and colleagues, who found that vSTM capacity *K* was associated with the microstructure of posterior thalamic radiations (Menegaux et al., 2017) and the structural connectivity of posterior thalamus to occipital cortices (Menegaux et al., 2019) in healthy young individuals. Nevertheless, the association between vSTM capacity and posterior thalamo-cortical connectivity in aging has not yet been investigated expressly.

Aging-related volumetric changes have been well documented (Courchesne et al., 2000; Ge et al., 2002; Raz and Rodrigue, 2006). Indeed, it has been shown that aging is accompanied by widespread reductions of grey-matter (GM) volume and increases in cerebrospinal fluid (CSF) starting in early adulthood (Salat et al., 2011; Walhovd et al., 2011). However, age-related changes in WM volume follow a complex trajectory. Several studies have found an increase in WM volume until the fourth or fifth decade of life, interpreted as ongoing myelination (Courchesne et al., 2000; Ge et al., 2002; Bartzokis et al., 2004), followed by a decrease that accelerates in late adulthood (Courchesne et al., 2000; Raz et al., 2005). However, volumetric studies do not provide information regarding the mechanisms responsible for those age-related WM changes. Diffusion tensor imaging, by contrast, allows inferences about WM microstructure by quantifying the magnitude and directionality of water diffusion in tissues (Pierpaoli and Basser, 1996; Pierpaoli et al., 1996). By the use of a tensor, a 3×3 matrix, diffusion in all three dimensions can be quantified and several measures derived. These include fractional anisotropy (FA), which describes how directional diffusion is (Basser, 1995), mean diffusivity (MD), radial diffusivity (RD), which represents the diffusivity perpendicular to fibers, and axial diffusivity (AD), which represents the diffusion parallel to the fibers. Predominant findings on age-related WM diffusivity changes have been decreased FA and increased MD in widespread tracts, including the inferior fronto-occipital fasciculus, sagittal stratum and posterior thalamic radiations in cross-sectional (Pfefferbaum, 2000; O'Sullivan et al., 2001; Malloy et al., 2007; Hugenschmidt et al., 2008; Vernooij et al., 2008; Westlye et al., 2010, Bennett et al., 2010; for review see Wozniak and Lim, 2006; Fama and Sullivan, 2015) and longitudinal studies (Barrick et al., 2010; Teipel et al., 2010). Furthermore, while it has been repeatedly reported that RD increases with aging (Baghat and Beaulieu, 2004; Zhang et al., 2010a; Bennett et al., 2010), findings on AD where more mixed and both increases and decreases have been reported (Zahr et al., 2009; Bennett et al., 2010; Sullivan et al., 2010a, 2010b; Burzynska et al., 2010). Interestingly, particularly in posterior thalamic areas, changes in RD and AD have been reported with aging (Kumar et al., 2013) and alterations in thalamo-cortical projections' volume have been found (Hughes et al., 2012).

Those changes in WM diffusivity with aging likely reflect microstructural alterations such as increase of brain water content, disruption of axon structure, myelin alterations or rarefaction of fibers (Minati et al., 2007). Indeed, post-mortem histological studies on human and rhesus monkeys brains have reported both a loss of myelinated fibers as well as a decrease in total myelinated fiber length in aging brains (Meier-Ruge et al., 1992; Marner et al., 2003). Further studies on rhesus monkeys' brains have reported age-related alterations in myelin sheaths of myelinated nerve fibers (Peters et al., 2001, 2002). Indeed, they reported that, although demyelination occurs in aging monkey brains, the overall myelin thickness is increased due primarily to remyelination processes and increase in the number of oligodendrocytes (Peters et al., 2009). However, in the process of remyelination by new oligodendrocytes, shorter internodal segments are produced, thus leading to a reduction in conduction velocity of the axons and, thus of changes in the timing in neuronal circuits Wang et al. (2005); for similar results in mice see Lasiene et al. (2008). Given the pronounced WM diffusivity changes, particularly in posterior thalamic areas and the myelin sheath alterations leading to conduction reductions and changes in timing in neural circuits, investigating the role of posterior thalamic connections in age-related vSTM capacity would appear highly relevant. It is known for instance from Menegaux and colleagues (Menegaux et al., 2017) that when

changes in white matter occur, the relationship between WM connectivity and VSTM capacity can change. Indeed, in preterm born adults, in whom thalamo-cortical microstructure and connectivity has been shown to be impaired compared to term-born individuals, the association between posterior thalamic radiations microstructure and vSTM capacity was changed compared to term-born individuals. Similar changes in the relationship between cognitive functions and WM integrity might also be found in other conditions affecting WM diffusivity, such as normal aging. Thus, we investigated whether the association between the structural connectivity of posterior thalamus to occipital cortices and vSTM capacity is similar throughout the lifespan or whether it varies as a function of age.

In order to examine this question, healthy individuals, aged 18–77 years, underwent both diffusion-weighted imaging and a TVA-based whole-report task of briefly presented letter arrays. Structural connectivity values were obtained by performing probabilistic tractography on DWI scans from occipital cortices to posterior thalamus, separately for each hemisphere. Estimates of vSTM capacity parameter *K* were derived from verbal letter report of the whole-report task. The relationship between the structural connectivity of posterior thalamus to occipital cortices (PT-OC), as defined by the mean PT-OC connection probability and vSTM capacity was analyzed by means of regression and partial correlation analyses.

2. Material and methods

2.1. Participants

The present study included 66 healthy adults aged 20–77 years, 32 of whom were females (mean age: 48.8 ± 19.6 years; mean school education 12.1 ± 1.6 years; Table 1). The distribution of participants across age was as follows: 22 participants below the age of 35 years, 19 participants between the age of 35 and 60 years and 25 participants above the age of 60 years. 60 participants were right-handed, 4 were left-handed and 2 were ambidextrous according to the Edinburgh Handedness Inventory (Oldfield, 1971). Written informed consent was obtained from all participants and the study was approved by the ethics committees of the Psychology Department of the Ludwig Maximilians Universität München (LMU Munich) and the Medical Department of the Technische Universität München (TUM). Initially, 108 adults (aged 19–78 years) of the Munich INDIREA aging cohort were recruited for the study. The Mini Mental State Examination (MMSE; Folstein et al., 1975) was used as screening for cognitive impairments in participants aged 60 years and above (i.e., a MMSE score below 27), and the Beck Depression Inventory (BDI; Beck et al., 1996) for screening for symptoms of depression in all participants (i.e., a BDI score above 19). From the original cohort, eleven participants dropped out before participating in all sessions, three participants were excluded because of high BDI test scores, one because of a low MMSE score, two because of uncorrected visual acuity deficits, five because of too low accuracy in the whole-report task, ten due to artifacts in their diffusion-weighted imaging data, two because of incomplete diffusion-weighted imaging datasets and eight participants for failing to undergo diffusion-weighted imaging assessment. A description of excluded participants can be found in Supplementary Material Table S1. All of the 66 remaining participants had no previous or current psychiatric (e.g., anxiety disorder, schizophrenia) or neurological conditions (e.g., brain injury, stroke), diabetes, or depression. Diffusion-weighted imaging was performed during one session at the Department of Neuroradiology of the TUM Klinikum rechts der Isar. In a separate, psychophysical-testing session at the Department of Psychology of the LMU Munich, visual attention functioning was assessed using the whole-report task. Event-related EEG potentials were also recorded during the task, but not analyzed for the current study. Additionally, participants completed the MMSE, and filled out demographic and BDI questionnaires. The average time between sessions was 2.6 months.

Table 1
Sample characteristics.

Variable	N = 66		
	M	SD	Range
Gender (F/M)	32/34		
Handedness (R/L/B)	60/4/2		
Education (years)	12.1	1.7	8.5–14.0
Age (years)	48.8	19.6	20–77
K (elements)	3.22	0.39	2.29–3.83
C (elements/s)	23.26	8.41	9.71–47.01
t0 (ms)	12.82	13.93	0.00–67.13
Crystallized IQ	102.1	16.6	72.5–140.0

2.2. TVA-based behavioural assessment of vSTM capacity

2.2.1. General assessment procedure

The whole-report task was conducted in a dimly-lit, sound-attenuated chamber (Industrial Acoustics Company) with simultaneous EEG recording. Stimuli were presented to participants on a 24″ LED screen (800 × 600 pixel resolution, 100-Hz refresh rate) at a distance of 65 cm.

Due to the special requirements of event-related components assessment, some of the experimental trials in the whole report task were repeated more often than others. Furthermore, for the event-related EEG assessment, it was also necessary to ensure balanced visual stimulation in both hemifields in the whole-report task. Thus, symbols were presented in the visual hemifield opposite to the target stimuli. These specific manipulations, however, do not affect the TVA parameters derived from fitting report accuracy in the different conditions.

Each participant completed a session of 1.5–2 h in duration, which included EEG preparation, presentation of written instructions and stimuli used in the experiment, a procedure for adjustment of the individual exposure durations and approximately 45 min of testing procedure.

At the beginning of each trial, a fixation point (a white circle, 0.9° of visual angle in diameter with a white dot in the center) was presented in the center of the display for a duration randomly drawn from 10 to 240 ms. Participants were instructed to fixate this point throughout the whole trial blocks. Subsequently, red and/or blue letters were briefly presented on a black background. Letters' exposure durations were determined individually for each participant in a preceding short practice session, so as to ensure a comparable level of task difficulty across participants. The letters were randomly chosen from the following set {A, B, D, E, F, G, H, J, K, L, M, N, O, P, R, S, T, V, X, Z} and appeared only once in a given trial. After stimulus presentation, a white question mark appeared in the center of the screen, indicating the start of verbal letter report. Participants could perform the verbal report of individual letters in arbitrary order and without stress on response speed. In order to avoid too much guessing, participants were instructed to report only letters they were fairly certain they had seen. Following each block, participants received feedback related to the accuracy of the letters they reported and not related to the overall performance level reached in the task. The desired range of 70–90% was indicated by green color coding on a report accuracy chart. In order to avoid too liberal or too conservative responding, participants were instructed by the experimenter to try to refrain from guessing and report only the letters he/she was relatively sure to have seen when accuracy dropped below 70%, and to try to name more letters (i.e., to be less anxious to report wrong letters) when it reached 90%. During the whole- (and the partial-) report task, the experimenter was seated behind the participant, entered the letters reported by the participant on a keyboard and manually started the next trial by a key press.

2.2.2. Whole-report task

On each trial, four letters were briefly presented on an imaginary semi-circle with a radius of 5.27° of the visual angle on either the left or the right of a central fixation point, and participants were instructed to

report orally as many of them as possible. Four blue symbols (composed of random letter parts; see Fig. 1) of the same luminance were displayed on the symmetrical semicircle on the other side of fixation. Diameters of letters and symbols were 1.3° of visual angle. At the beginning of each block of trials, a white arrow pointed towards the side on which the report-relevant stimuli would appear in this block. The target side in the first block was counterbalanced across participants and then alternated throughout the experiment. Seven conditions were used. In five conditions, the stimulus array was followed by masks (see Fig. 1), which consisted of eight red-blue scattered squares (of side length 1.3° of visual angle) that appeared at each stimulus location for a duration of 900 ms. In two unmasked conditions, stimuli were followed by a blank screen with a fixation point shown for 900 ms. The masked letter arrays were presented for five different, individually adjusted exposure durations. In addition, as mentioned above, two unmasked conditions were used, one with the second shortest exposure duration and one with an exposure duration of 200 ms. In the unmasked conditions, the exposure durations are effectively prolonged compared to masked conditions due to visual persistence of the stimulus array (Sperling, 1960). Thus, the five masked conditions and two unmasked conditions resulted in seven different effective exposure durations. Different experimental conditions were equally distributed across blocks of trials and were displayed in randomized order within each block (Fig. 1).

On the top row in the middle, the regions of interest derived from the NTVA model of Bundesen are shown. Red represents the occipital cortex; the whole thalamus is shown in blue and the posterior thalamus in green. In the top left corner, a 3D representation of probabilistic tractography between the left occipital cortex and the left thalamus is shown for one individual. The top right corner shows an example of an individual's FA image modulated by his V1 map which is the principal eigenvector of the tensor. On this modulated FA image, WM tracts with a left-right orientation are shown in red, tracts with an antero-posterior orientation in green and tracts with an up-down orientation in blue. In the bottom left corner, an example of the whole-report task is shown. At the beginning of each trial, a fixation point was presented in the center of the display for a duration randomly drawn from 10 to 250 ms. Then the letters are presented in on hemifield for 5 different exposure duration previously determined during a test phase. Stimuli presentation as either followed by masks or blank screen presentation before the participant was asked to verbally report the letters. In the bottom right corner, a vSTM capacity *K* fit is presented for one subject.

The exposure adjustment phase consisted of 48 trials divided into 4 blocks of twelve triples of trials. Each triple consisted of two trials that were not used for adjustment, but simply for familiarizing the participant with the task. These were either unmasked trials with an exposure duration of 200 ms, or masked ones with an exposure duration of 250 ms. One trial in each triple was used for adjustment; this was masked and initially displayed for 80 ms. Each time the participant reported at least one correct letter in this trial, exposure duration was decreased by 10 ms until the lowest exposure duration was identified. Based on this value, a set of 4 additional exposure durations was chosen from the predefined sets. The testing phase consisted of 10 experimental blocks, each including 40 trials. There were 30 trials for each exposure duration (with the exception of the condition with unmasked trials presented for 200

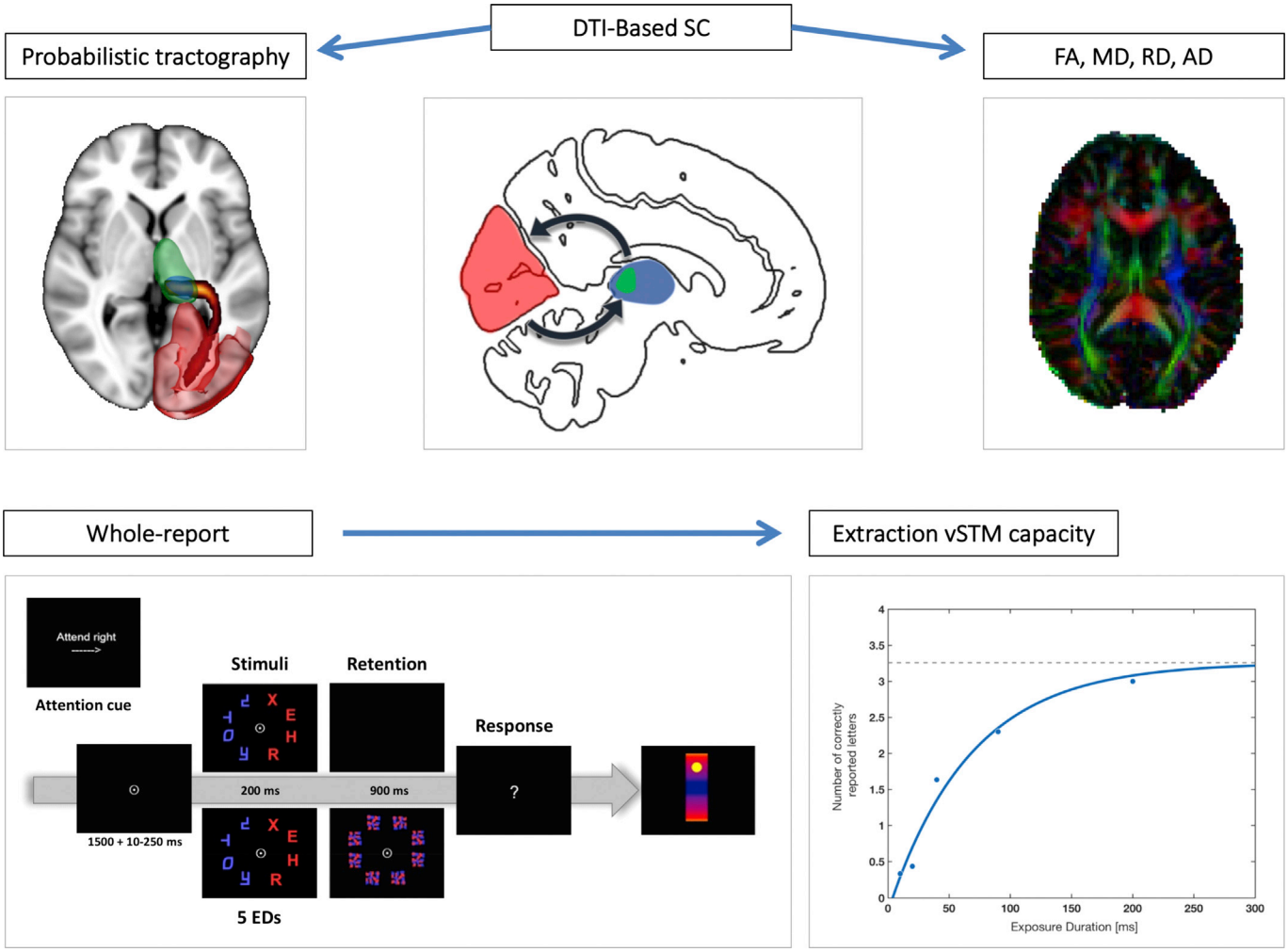

Fig. 1. Presentation of the model, task and methods used in our study.

ms, for which 220 trials were presented (these trials were critical for ERP analysis).

2.2.3. Estimation of visual short term memory capacity

Modeling of individual participant's vSTM capacity was based on the TVA computational model implemented in the libTVA toolbox for Matlab (Mads Dyrholm, www.machlea.com/mads/libtva.html). Detailed descriptions of the fitting procedure can be found in Dyrholm et al. (2011). The TVA-based whole-report fitting procedure models the probability of correct letter report in terms of an exponential growth function with increasing (effective) exposure duration. The variation of exposure duration (7 durations) was intended to generate a broad range of performance which specified the whole probability distribution of the number of correctly reported elements as a function of the effective exposure duration. The asymptote of the function represents vSTM capacity or parameter *K*, which indicates the maximum number of elements that can be simultaneously represented in vSTM. Along with parameter *K*, three additional parameters which are of no particular interest for the question at issue in the present study were estimated (estimating these is part of the fitting procedure): visual processing speed (parameter *C*), that is, the rate of visual information uptake (in elements per second) which is given by the slope of the growth function at its origin; perceptual threshold (parameter t_0) which indicates the visual perceptual threshold, that is, the longest ineffective exposure duration (in ms) below which information uptake is effectively zero; and parameter μ, representing the prolongation of the effective exposure duration (in ms) on unmasked trials. For participants whose t0 was estimated to be below 0 (9 out of 66), we refitted the data fixing t0 at 0. This new fit did not modify the mean value of K and C parameters (Supplementary Table S2) nor any analyses in this study (Supplementary Table S3 and Supplementary Fig. S1).

2.3. Imaging data acquisition and preprocessing

2.3.1. Imaging data acquisition

Whole brain T1-and diffusion-weighted imaging data were acquired on a 3T Philips Ingenia scanner with a 32 channel head coil and a SENSE factor of 2. Diffusion images were acquired using a single-shot spin-echo echo-planar imaging sequence, resulting in one non-diffusion weighted image (b = 0 s/mm2) and 32 diffusion weighted images (b = 800 s/mm^2, 32 non-collinear gradient directions) covering whole brain with: echo time (TE) = 61 ms, repetition time (TR) = 14206.980 ms, flip angle = 90°, field of view = 224 × 224 mm^2, matrix = 112 × 112, 60 transverse slices, voxel size = 2 × 2 × 2 mm^3. A whole head high-resolution T1-weighted anatomical volume was acquired using a 3D magnetization prepared rapid acquisition gradient echo sequence with the following parameters: repetition time = 9 ms; time to echo = 4 ms; inversion time, TI = 0 ms; flip angle = 8°; 170 sagittal slices; field of view = 240 × 240 mm^2; matrix size = 240 × 240; reconstructed voxel size = 1 × 1 × 1 mm^3.

2.3.2. Quality check

All acquired MRI images were visually inspected by two independent raters (A.M., A.V.) for excessive head motion, and apparent or aberrant artifacts. In addition to visual inspection of the raw data and preprocessed data, we also used the fitting residuals (the sum-of-squared-error maps generated by DTIFIT) to identify data corrupted by artifacts. Artifacts include motion-induced artifacts, insufficient fat suppression (ghosting) artifacts, and extreme distortion artifacts, which led to the exclusion of ten participants overall. Furthermore, Fluid-attenuated inversion recovery images were acquired as part of the standard MRI protocol of the Klinikum Rechts der Isar and examined by experienced radiologists to exclude potential lesions and WM abnormalities.

2.3.3. Preprocessing

Diffusion data preprocessing was performed using FMRIB Diffusion Toolbox in the FSL software (www.fmrib.ox.ac.uk/fsl; Jenkinson et al., 2012) after converting data from DICOM to niftii format using micron dcm2nii (Rorden et al., 2007) as described in previous work (Meng et al., 2015). All diffusion-weighted images were corrected for eddy current and head motion by registering all diffusion weighted volumes to theb0 image and skull and non-brain tissue were removed using the Brain Extraction Tool (BET). The tensor model was then applied voxel by voxel using the tensor model fit (Smith et al., 2004) in order to obtain voxel-wise FA and MD maps. Lambda 1, lambda 2 and lambda 3 maps, the three eigenvalues of the tensor representing the length of the eigenvectors, were also obtained from the tensor fitting procedure. They were used to calculate RD and AD maps. RD maps were obtained by averaging lambda 2 and lambda 3 maps and AD by renaming lambda 1 maps.

T1-weighted images were preprocessed using the anatomical processing script from FSL, which included reorientation, image cropping, bias field correction, linear (FLIRT, FMRIB's Linear Image Registration Tool) and non-linear (FNIRT, FMRIB's Non-Linear Image Registration Tool) registration to the MNI standard space. Non-linear transformation output included a structural–to-MNI standard space warp field and its inverse (MNI-to-structural). Preprocessing also included brain extraction using BET and both tissue type and subcortical structure segmentations that were used to register diffusion-weighted images to preprocessed structural T1-weighted images using boundary-based registration for echo planar imaging data, thus yielding a diffusion-to-structural transformation matrix. In order to register diffusion-weighted data to the MNI 152 template via structural scan, we combined the previously generated structural-to-MNI non-linear transformation matrix with the diffusion-to-structural transformation matrix, thus resulting in a diffusion-to-standard space transformation. This transformation was used in a later step to transform the individual fdt_paths, the 3D image file containing the output connectivity distribution to the seed mask, to standard space.

2.3.4. Probabilistic tractography

2.3.4.1. Regions of interest (ROI) generation. We used the MNI 152 2-mm label atlas combined with the Harvard Oxford 2-mm cortical atlas to create the cortical occipital masks in standard space. Masks of the right and left posterior thalamus containing pulvinar nuclei were created from the Talairach atlas. Whole-brain left and right hemisphere masks were also created from the MNI 152 2 mm atlas and used as exclusion masks in the tractography process. All masks were transformed into the participants' native space using the reverse non-linear mapping previously obtained and nearest neighbour interpolation.

2.3.4.2. Estimation of diffusion parameters and probabilistic tractography.- Using the FDT toolbox from FSL, we first ran the function of Bayesian estimation of diffusion parameters obtained using sampling techniques (BedpostX) for each participant. It estimates the individual diffusion parameters at each voxel while considering the number of crossing fibers per voxel (Behrens et al., 2003, 2007). We used the default parameters implemented in FDT: 2 fibers per voxel, weight of 1 and burning period 1000. Using the previously created ROIs (as described above), tractography was run for each hemisphere with the occipital ROI as seed and the posterior thalamus as waypoint target mask using the probtrackx2 function from FSL. We also used an exclusion mask from the opposite hemisphere in order to ensure the ipsilateral nature of the tractography. We performed tractography separately from each occipital ROI to the posterior thalamus. For each participant, 5000 streamlines were initiated per seed voxel with a path length of 2000 × 0.5 mm steps, a curvature threshold of 80° and loop checking criteria. The resulting image or fdt_paths represents the path connecting the seed region to the target, where the value in each voxel represents the number of streamlines generated from the seed region that pass through that voxel. Due to the

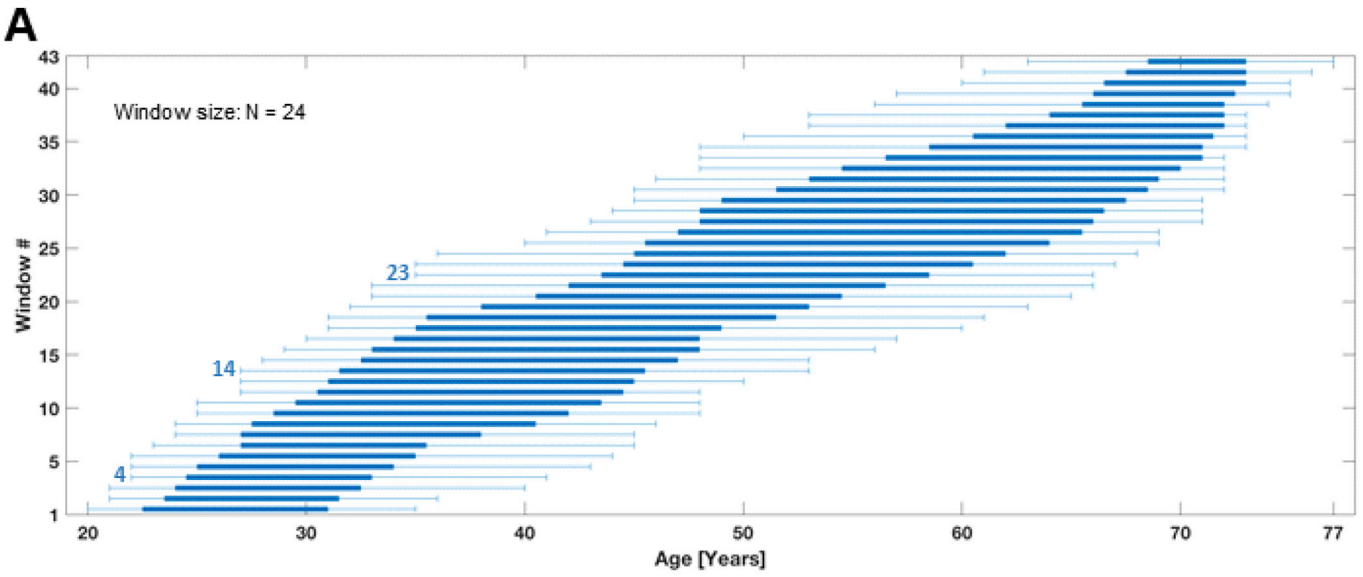

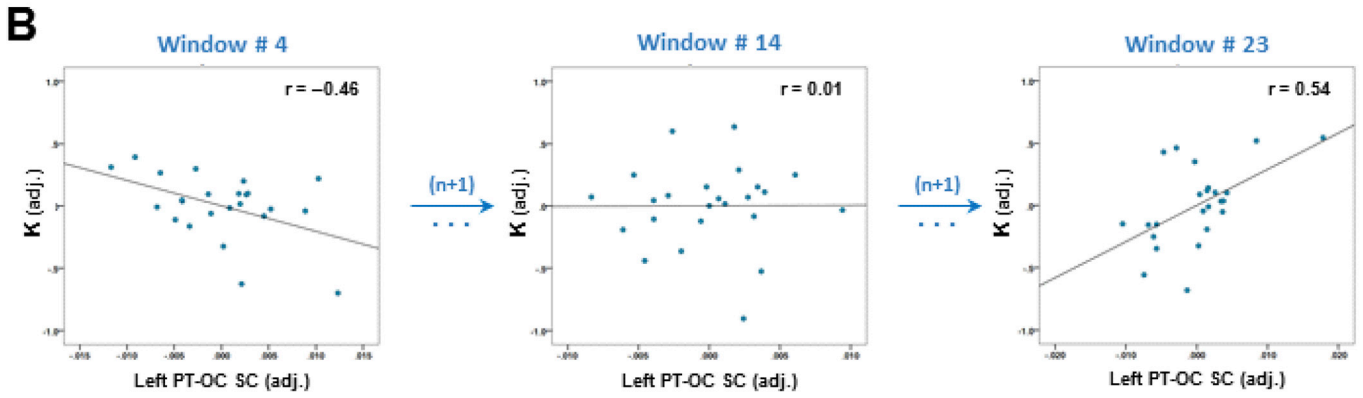

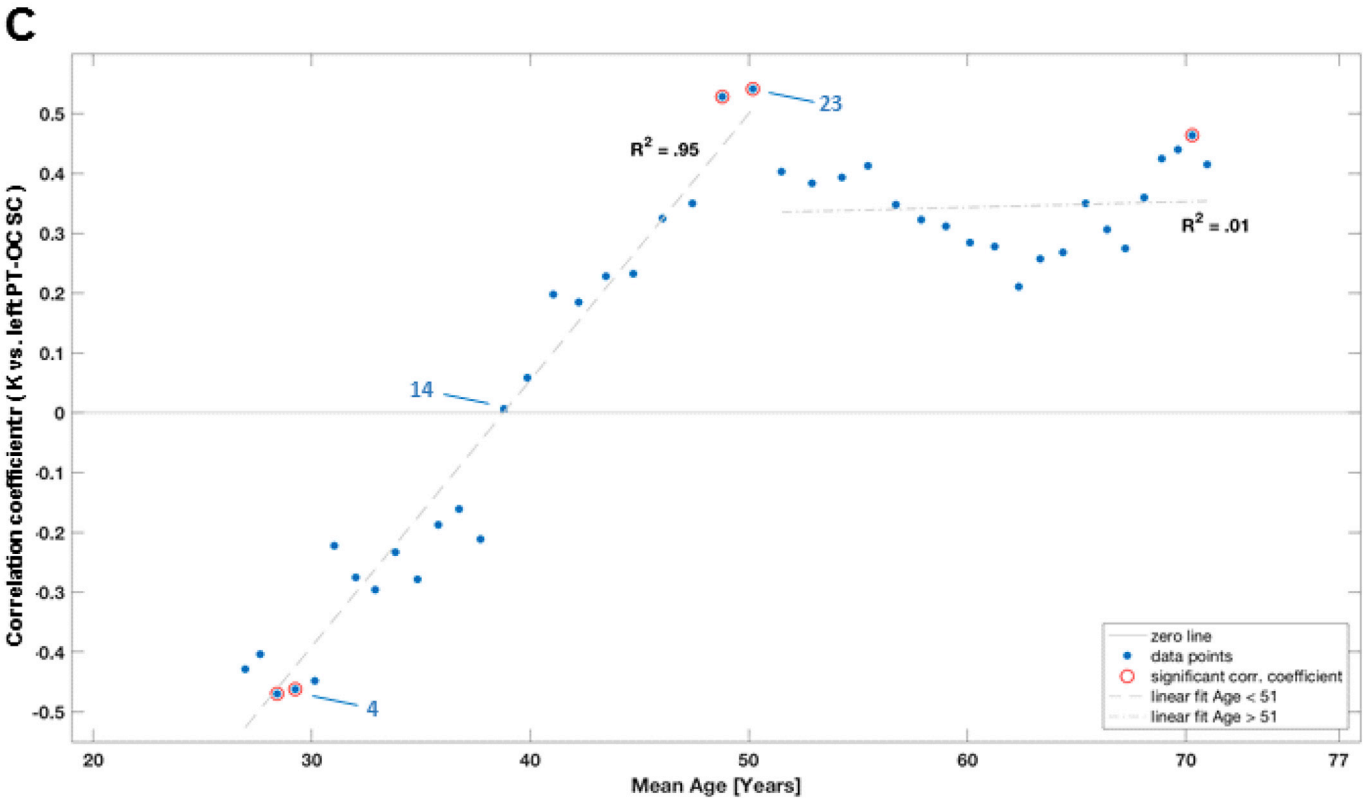

(caption on next page)

differences in volume of each area across participants, we normalized the resulting tract estimates (fdt_paths) by dividing them by the waytotal (total number of streamlines generated from the seed region that reaches the target region; Rilling et al., 2008), thus resulting in a probability map of connectivity (Zhang et al., 2010b; Arnold et al., 2012; Behrens et al., 2007; for review, see Jbabdi et al., 2015). These probability maps were then transformed back into standard space so they can be used for statistical analysis (Fig. 1).

2.4. Extraction of FA, MD, AD, and RD maps from path probability maps

Native FA, MD, AD and RD maps were transformed into standard space using the nonlinear transformation described previously. A mask of the tracts between posterior thalamus and occipital cortex for the left and right hemispheres was obtained using the individual fdt_paths maps from probtrackx transformed to standard space. The average paths of our cohort for left and right PT-OC tracts were calculated with fslmaths and thresholded above 0.03. The average left and right tract masks were then binarized before being used to extract the mean FA MD, RD and AD values for each participant using the fslmeants command. In a similar manner, we extracted the mean connectivity value of all the voxels of left and right tracts (respectively left PT-OC tract mean connectivity and right PT-OC tract mean connectivity).

2.5. Estimation of tissue type and total intracranial volumes

In order to obtain volumetric measurements for the whole brain, T1 images were segmented into GM, WM and CSF tissue classes and normalized to the MNI 152 mm template using DARTEL (SPM12 software package, http://www.fil.ion.ucl.ac.uk). The segmented and normalized images were modulated to account for the structural changes resulting from the normalization process, thus indicating GM, WM and CSF volume. Grey- and white-matter images were smoothed with an 8 mm full-width at half-maximum filter (FWHM). Total intracranial volume was estimated by first computing and then adding up the totals (in liters) of the warped, modulated and smoothed GM, WM and CSF segments with the in-built SPM Tissue Volumes Utility (Malone et al., 2015).

2.6. Statistical analysis

For each individual connection probability map of posterior thalamus previously normalized and transformed into standard space, the mean probability of connection was extracted for each hemisphere, thus yielding the left and right PT-OC connection probabilities. These values were then used to investigate the role of left and right PT-OC structural connectivity in the reduction of vSTM capacity with aging, using a regression model with vSTM capacity as dependent variable and age, PT-OC connection probability and interaction between both variables as independent variables. Gender, handedness, CSF and crystallized IQ were also included as covariates in the model. The effect of age on GM, WM and CSF volume was analyzed using Pearson correlation. All analyses were carried out using the SPSS statistics package version 21 (IBM).

2.7. Sliding window analysis

In order to investigate in greater depth the association between vSTM capacity and left PT-OC connection probability with age, we used a sliding window approach: Participants were sorted according to age. The sliding window contained a subgroup of 24 participants: The association between vSTM capacity and left PT-OC connection probability was calculated by Pearson partial correlation in this subgroup, controlling for age, gender, handedness, IQ and CSF. The window was then consecutively shifted by one participant to get an 'older' group of 24 subjects and the partial correlation repeated for each shift. In Fig. 2, the mean age of the sliding window subgroup versus the correlation coefficient of the partial correlation is represented (See Fig. 2A).

In order to test the reliability of the sliding window analysis, we performed bootstrapping analyses. We repeated the analysis sequentially by excluding each participant separately once, to test whether outliers might have influenced the results. We found a very similar pattern, suggesting that the results were not driven by non-representative outliers (see Supplementary Material Fig. S2B). We then repeated the sliding window analysis for different window sizes, varying from 20 to 35 subjects, and found a congruent pattern of results, which suggested that the results are reliable and do not depend on the selected window size (Supplementary Material Fig. S2A).

2.8. Control analyses

In order to test the structural specificity of our connectivity results for the occipital region, we performed tractography from the left and right motor cortices as control ROIs to the thalamus. We used Brodmann areas 4a, 4p, and B6 from the Jülich atlas, separately for each hemisphere, combined with the Harvard-Oxford 2-mm cortical atlas to create the cortical motor masks for the left and the right hemisphere. The Oxford thalamic 30% 2-mm connectivity atlas was used (Behrens et al., 2003) to create masks for left and right thalami. For each individual connection probability map between the left or right motor cortex (MC) and the left or right thalamus, posterior thalamus masks of each hemisphere were used to extract the mean probability of connection from these regions. To investigate the role of left or right PT-MC structural connectivity in the reduction of vSTM capacity with aging, the same multiple linear regression model as previously described was used.

Furthermore, in order to test the cognitive specificity of our results for vSTM capacity *K,* we analyzed the association between left and right PT-OC connection probability and the additional TVA parameters that can be extracted from the whole report task (i.e. processing speed *C* and perceptual threshold *t0*). Both parameters were linked to left or right PT-OC connection probability via multiple linear regression using the same model as described above. These latter analyses on parameters of no particular interest in our study mainly served for the documentation that potential relations between PT-OC and vSTM capacity do not result from underlying relationships with parameters of visual threshold or processing speed.

2.9. Data availability statement

Participants data used in this study are not publicly available but can be made available by the corresponding author upon request.

3. Results

3.1. Aging moderates the association between PT-OC structural connectivity and vSTM capacity

In order to test whether our sample was representative with respect to brain changes that are normally displayed by aging individuals and in order to identify variables that needed to be used as control variables in

Fig. 2. Aging moderates the association between vSTM capacity and the structural connectivity (SC) of left posterior thalamus to left occipital cortex.
A illustrates the sliding-window approach used in the current study: participants were ranked by age and the first 24 individuals constituted the first window which was shifted consecutively by one participant. In **B,** three examples of correlations between vSTM capacity parameter *K* and left PT-OC SC in different age windows as indicated in (A) are shown. The correlation coefficient r is presented in the upper right corner of the individual plots. In **C**, these correlation coefficients are plotted against the mean age of the window group. Significant correlations between K and left PT-OC SC are indicated with a red circle, the dotted lines represent linear fits.

the later analyses, we first assessed age-related differences in brain structure, specifically: on brain volume. Using voxel-based morphometry, we found that WM volume did not significantly vary as a function of age ($r = -0.04$; $p = .73$) while CSF volume was significantly increased ($r = 0.79$; $p < .001$) and GM volume significantly reduced ($r = -0.57$; $p < .001$). As this pattern is similar to that observed in previous studies (Salat et al., 1999, 2011; Walhovd et al., 2011), we can conclude that individual differences in brain structure in our sample are representative of those that are to be expected in healthy aging individuals.

In order to investigate the role of PT-OC structural connectivity in the reduction of vSTM capacity with aging, a regression model with Age, PT-OC connection probability and interaction between both variables, Gender, Handedness, IQ and CSF was used. The last four variables were included in the model in order to control for gender, handedness, general cognitive performance, and brain volume effects. We tested the model for left and right PT-OC connectivity separately, in order to account for potential side effects of age as suggested by previous studies (Silver et al., 1997; Huster et al., 2009; Johnson et al., 2014). Concerning right PT-OC connectivity, we found that the model was not a significant predictor of vSTM capacity $F(7.58) = 2.25$; $p = .087$. We therefore did not further examine this model. Concerning left PT-OC connectivity, we found that the overall model was a significant predictor of (23.8% of variance in) vSTM capacity, demonstrating the reliability of this model to explain age-related variance in vSTM capacity (Table 2). In accordance with previous studies (McAvinue et al., 2012; Wiegand et al., 2014a, 2014b) we found vSTM storage capacity *K* to decline with increasing age in our participant group ($\beta 1 = -0.047$; $p = .001$). We then aimed to investigate whether PT-OC structural connectivity was associated with vSTM, as suggested by the NTVA and previous findings (Menegaux et al., 2017). We found left PT-OC connection probability to be significantly associated with vSTM capacity ($\beta 2 = -42.370$; $p = .032$). Finally, we tested whether the association between PT-OC structural connectivity and vSTM capacity *K* varied as a function of age. We found a significant interaction between Age x left PT-OC connection probability ($\beta 3 = 0.952$; $p = .009$), demonstrating that age modifies the relationship between PT-OC structural connectivity and vSTM capacity.

3.2. Control analyses

3.2.1. Analysis of cortical specificity: vSTM capacity is not associated with posterior thalamus-motor cortex structural connectivity

In order to test the cortical specificity of the association between PT-OC structural connectivity and vSTM capacity, we investigated whether vSTM storage capacity would also be associated with the structural connectivity of the posterior thalamus to other cortical ROIs such as the left and the right motor cortex (MC). Using the same regression model as above, we found that neither the left $F(7.58) = 2.25$; $p = .255$ nor the right PT-MC structural connectivity $F(7.58) = 2.25$; $p = .157$ were significantly associated with vSTM capacity (see Supplementary Tables S4 and S5).

Table 2
Regression table Coefficients of multiple linear regression for vSTM capacity and left PT-OC connection probability.

Independent variables	Dependent variable = vSTM capacity		
	β values	P value	95% CI
Age	**−0.047**	**.001**	[−0.075, −0.020]
Left PT-OC structural connectivity	**−42.4**	**.032**	[−81.1, −3.7]
Interaction Age x left PT-OC Structural connectivity	**0.95**	**.009**	[0.243, 1.661]
Gender	−0.05	.609	[−0.261, 0.155]
Handedness	−0.16	.180	[−0.400, 0.077]
IQ	**0.008**	**.019**	[0.001, 0.015]
CSF	2.16	.063	[−0.12, 4.43]

3.2.2. Analyses of functional specificity: PT-OC structural connectivity is not associated with processing speed or perceptual threshold

In order to test whether the results obtained for vSTM storage capacity *K* were cognitively specific, we additionally investigated whether left- or right-hemisphere PT-OC connection probability predicted other TVA parameters visual processing speed *C* and perceptual threshold *t0* using the same regression model as previously. We found that neither left nor right PT-OC structural connectivity were significantly associated with processing speed ($F(7.58) = 2.25$; $p = .100$; $F(7.58) = 2.25$; $p = .172$ respectively, see Supplementary Tables S6 and S7) nor perceptual threshold ($F(7.58) = 2.25$; $p = .208$; $F(7.58) = 2.25$; $p = .251$ respectively, see Supplementary Tables S8 and S9).

3.3. The effect of age on the association between left PT-OC structural connectivity and vSTM capacity: shift and alteration of microstructure

In order to investigate the association between PT-OC connection probability and vSTM capacity with increasing age in more depth, we applied a sliding window approach. This allowed tracking the association between PT-OC connectivity and vSTM capacity as a pseudo-continuous function of age. The window was slid until the age of 77 years (the oldest participant's age), resulting in the plot presented in Fig. 2C. We found that the association between vSTM capacity and left PT-OC structural connectivity was linearly reversing from a negative association in the youngest groups to a positive association around an age of 50 years. Up from this age, the positive association remained significant throughout. As illustrated in Fig. 2B, window number 4, we found that in young individuals with a mean age of 28 years, vSTM capacity *K* was significantly negatively correlated with left PT-OC structural connectivity ($r = -0.46$; $p < .05$); by contrast, in individuals with a mean age of 50 years (see window 14 in Fig. 2), it was significantly positively correlated with left PT-OC structural connectivity ($r = 0.54$; $p < .05$). Similarly, we found that for individuals with a mean age of 70 years, vSTM capacity was significantly positively associated with left PT-OC structural connectivity ($r = 0.45$; $p < .05$).

This reverse association between vSTM capacity and left PT-OC connection probability in younger compared to older individuals was somewhat surprising. Considering this finding, the well-known effects of aging on WM microstructure (Pfefferbaum et al., 2000; Hugenschmidt et al., 2008; Westlye et al., 2010) and previous studies suggesting that WM microstructure mediates the impact of age on attention functions (Salami et al., 2012), we conjectured that the reverse association to vSTM capacity that we found might be caused by changes in WM properties of left PT-OC tracts. Thus, we first investigated whether the microstructure of the tracts connecting the left posterior thalamus to the left occipital cortex was altered with increasing age. We found that the mean FA of these tracts was significantly reduced with increasing age ($r = -0.54$; $p < .001$) while MD was significantly increased ($r = 0.63$; $p < .001$). Similarly, RD and AD were also significantly increased with age ($r = 0.60$; $p < .001$; $r = 0.36$; $p = .003$ respectively) (see Supplementary Fig. S3). We then investigated the association between FA/MD from left PT-OC tract and left PT-OC connection probability and found that neither FA nor MD values were significantly correlated with left PT-OC connection probability ($r = -0.13$; $p = .31$ and $r = -0.06$; $p = .65$ respectively). Then we investigated whether these values might be indirectly related to each other by extracting the mean connectivity value of all the voxels of the tract between left occipital cortex and left posterior thalamus (i.e excluding posterior thalamus). Interestingly, when looking at the association between left FA and left PT-OC tract mean connectivity using the sliding window approach, we found that they seemed to be positively associated in the younger participants and significantly

negatively associated in older participants (see Supplementary Fig. S4), while in the whole sample the left PT-OC tract mean connectivity was positively associated with PT-OC connection probability ($r = 0.39$; $p = .002$; see Supplementary Fig. S5). This suggested that the relationship between microstructure and connectivity of PT-OC tract is complex and seems to be age dependent.

4. Discussion

Using a whole-report paradigm and TVA -based modeling together with probabilistic tractography in a group of healthy participants aged 20–77 years, we investigated age-related differences in the association between the structural connectivity of posterior thalamus to occipital cortices and vSTM capacity *K*. We found that the association between left PT-OC connection probability and vSTM capacity differed throughout the lifespan. Indeed, in younger individuals at an age below 30 years, vSTM capacity was significantly negatively associated with left PT-OC structural connectivity. In older individuals above the age of 50, this association was reversed, i.e. the higher the connection probability between left posterior thalamus and left occipital cortex, the higher the vSTM capacity *K*. When exploring the microstructural properties of the left PT-OC tracts, we found that FA was significantly decreased with age while MD, AD and RD were significantly increased. This suggests that age modifies the microstructural properties of the tracts connecting the left posterior thalamus to the left occipital cortex. Such changes might underlie the altered relationship between thalamo-cortical connectivity and vSTM capacity *K*. Altogether, to our knowledge; our findings provide the first evidence that aging not only impairs vSTM capacity *K* and the structural connectivity between posterior thalamus and occipital cortices, but also modifies the relationship between these measures.

4.1. Aging moderates the association between PT-OC structural connectivity and vSTM capacity

In order to investigate whether aging modified the association between vSTM capacity and PT-OC connection probability, we carried out two different analyses: a multiple regression with vSTM capacity as dependent variable and age, PT-OC connection probability and interaction between both variables as independent variables, as well as a sliding-window approach.

We found that left PT-OC connection probability was significantly associated with vSTM capacity. This is in line with the NTVA assumption that posterior thalamus and visual cortices are relevant for vSTM capacity. According to NTVA, the activity of visual neurons coding for objects that won the race for vSTM representation is assumed to be sustained and reactivated by a feedback loop gated by the thalamic reticular nucleus (Bundesen et al., 2005). Our finding of a significant association between vSTM capacity and PT-OC connection probability suggests that, independently of age, connections from posterior thalamus to occipital cortices are relevant for vSTM capacity. This finding complements the one from our previous study in which we used a subsample of this dataset and slightly different masks for tractography and found that vSTM capacity was significantly negatively associated with left PT-OC structural connectivity (Menegaux et al., 2019). Our finding of the relevance of PT-OC connections for vSTM capacity is also in agreement with those from Menegaux and colleagues (Menegaux et al., 2017) who found the microstructure of posterior thalamic radiations, as reflected by FA, to be significantly associated with vSTM capacity in a group of healthy young adults aged 26 years. Together, these findings suggest that tracts connecting posterior thalamus to occipital cortices and their microstructure are critical for vSTM capacity.

As mentioned in our previous study (Menegaux et al., 2019), the fact that we found the left and not the right PT-OC connection probability to be related to vSTM capacity might suggest that the left hemisphere plays a more important role for vSTM storage of objects than the right one. This is in agreement with the findings from a positron emission tomography study by Smith and colleagues (Smith et al., 1995) on the respective relevance of both hemispheres in visual-spatial vs. visual-object short--term storage which suggested the left-hemisphere to be specialized in object information while the right hemisphere was more relevant for vSTM spatial information. Moreover, a study from Todd and Marois (2005) using functional MRI, found that activity along the left intraparietal sulcus/intraoccipital sulcus was associated with individual differences in vSTM capacity. Finally, findings from a lesion-study by Finke and colleagues investigating the consequences of unilateral posterior parietal damage in humans suggested that a left-sided vSTM system might be specialized for the maintenance of visual object information (Finke et al., 2006). While, our results together with the findings of the previously mentioned studies suggest that PT-OC connectivity of the left hemisphere subserves vSTM capacity, the particular relevance of the left hemisphere might alternatively be related to the fact that we used letter stimuli that have to be verbally reported.

The main finding of the current study is the significant interaction effect between age and left PT-OC structural connectivity on vSTM capacity, which suggests that age moderates the association between PT-OC structural connectivity and vSTM capacity (Salthouse, 2011) This interaction effect remained significant when controlled for the potential effects of CSF volume and IQ. Modification of the association between vSTM capacity and a brain correlate, here PT-OC structural connectivity, with age had previously been suggested by electroencephalographic findings of a weaker association between vSTM capacity and contralateral delay activity in older compared to younger adults (Wiegand et al., 2014a; Sander et al., 2011; Duarte et al., 2013). It also fits with previous findings that, in populations with changes in WM connectivity, the association between vSTM capacity and posterior thalamic radiation microstructure might change compared to young healthy groups. In particular, these results fit to those from a previous study that used the same TVA-based methodology in preterm-born adults who are known to exhibit changes in thalamo-cortical connectivity (Menegaux et al., 2017). Indeed, Menegaux and colleagues found that the association between FA in posterior thalamic radiations and vSTM capacity was reversed in preterm compared to term-born adults (Menegaux et al., 2017). Arguably, modifications of thalamo-cortical tracts microstructure in older participants might also affect the association between thalamo-cortical connectivity and vSTM capacity *K*. However, although the significant interaction effect between age and left PT-OC connection probability on vSTM capacity suggests that aging modifies this structure–function association, it did not provide information regarding the direction of change. Thus, in order to investigate the direction of this interaction, we examined the association between vSTM capacity *K* and PT-OC connection probability as a pseudo-continuous function of age using a sliding-window approach. This yielded intriguing findings, in that it showed that the association between vSTM capacity *K* and PT-OC structural connectivity was continuously reversed from negative to positive with increasing age.

4.2. The association between vSTM capacity and left PT-OC structural connectivity is continuously reversed with age: Potentially relevant microstructural alterations

This continuum across aging suggests that there is a ceaseless process influencing PT-OC connectivity such that the association with vSTM capacity *K* is changed. Interestingly, it is well documented that aging affects WM microstructure (Pfefferbaum et al., 2000; Hugenschmidt et al., 2008; Westlye et al., 2010) and that WM microstructure can mediate the impact of age on attention functions (Salami et al., 2012). Accordingly, a change in WM microstructure could be the critical mechanism behind the continuous inversion from negative to positive of the association between vSTM capacity and left PT-OC structural connectivity. Thus we examined whether age-related microstructural changes of PT-OC tracts would be evident in our older participants. Interestingly, we found that FA in left PT-OC tracts was reduced and MD,

RD and AD increased in older compared to younger participants. These findings are in line with those of Kumar et al. (2013) who reported increased AD in bilateral posterior thalamic WM of older participants, and of Hugenschmidt et al. (2008) and Westlye et al. (2010) who found reduced FA in posterior thalamic radiations of older compared to younger adults. A reduced FA value might be interpreted as a decrease in the organization of WM caused by various processes such as demyelination, axonal degradation or gliosis (Beaulieu, 2002; Concha et al., 2006; Lebel et al., 2008; Assaf et al., 2008). The conjunction of decreased FA with increased MD, RD and AD is in line with findings from Burzynska et al. (2010) and would preferentially suggest a decrease in fiber organization which might be caused by axonal loss or gliosis (Beaulieu, 2002; Concha, 2006; Lebel, 2008 et Assaf, 2008).

In order to bring further answer to this hypothesis, we investigated whether FA and MD measures of left PT-OC tract was associated with left PT-OC connection probability. We found that these measures were not directly correlated with each other. However, they were both associated with the left PT-OC tract mean connectivity of the PT-OC tract. Furthermore, the association between the mean FA and PT-OC tract mean connectivity of the tract varied with age. Indeed, in young participants, higher FA was related to higher vSTM capacity, while in older participants this association was reversed. This illustrates indicates a complex nature of the relationship between FA and number of streamlines (reflected in the PT-OC tract mean connectivity value) which is also documented in several other studies. Indeed, a study by Khalsa and colleagues reported no association between FA and the number of streamlines for all fiber bundles studied but one were the association found was positive (Khalsa et al., 2014). This suggested that the association between both variables might be region dependent. Herting et al. (2013) investigated the association between both white matter microstructure and connectivity as measured using tensor estimation as well as deterministic tractography respectively, with aerobic fitness in male adolescents. They found that adolescents with high fitness had a higher number of streamlines compared to adolescents with low fitness but that FA was not different between groups. Together, these studies seem to suggest that number of streamlines and FA are not necessarily related to each other and thus that one cannot assume that higher number of streamlines reflects higher FA.

In our study we found that the relationship between connectivity and microstructure of PT-OC tract seems to vary with age. Indeed, in older participants, who showed lower FA than younger participants, we found that lower FA was associated with higher connectivity in the tract. Furthermore, in older participants, higher mean connectivity in the PT-OC tract was associated with higher PT-OC connection probability and higher PT-OC connection probability was associated with better vSTM capacity. It is important to remember that the number of streamlines generated by probtrackx does not necessarily reflects the underlying number of fibers (Jones et al., 2013). Nevertheless, it seems that in elderly people where the microstructure of PT-OC fibers is altered, the number of fibers connecting left posterior thalamus to left occipital cortex is particularly important for vSTM capacity and more fibers seems to be associated with better vSTM capacity. With respect to microstructure, a decrease in FA could reflect several processes such as reduction of fiber density or alterations in myelination as mentioned previously. Thus, we cannot ascertain that in our sample, a reduction of FA reflects alterations in myelination. Nevertheless, studies in non-human primates found that aging modified myelin thickness via processes of demyelination and remyelination by newly formed oligodendrocytes (Peters, 2009). Interestingly, they found that in the process of remyelination, shorter internodal segments are produced, thus leading to a reduction in conduction velocity of the axons and, thus of changes in the timing in neuronal circuits Wang et al. (2005); for similar results in mice see Lasiene et al. (2008). We therefore propose that the information transfer in the PT-OC tracts of the older participants is less optimal, probably due to changes in myelination and timing. Consequently, the conscious perception and storing of information in vSTM is impaired. Thus, it might be the case that particularly in older participants, a substantial number of fibers is needed, so that good information transfer is guaranteed and vSTM representations can be kept active in the PT-OC tract.

In younger participants the PT-OC fibers might have a higher conduction velocity and might, thus, be more efficient in keeping vSTM representations active. Therefore, the number of fibers in PT-OC tract might be less important for vSTM capacity and a lower number of fibers might even indicate particularly effective recurrent activation of vSTM representations in the PT-OC tract.

We did not investigate fronto-parietal tracts in our study and thus cannot contribute to the question of potential compensation via more frontal structures. However, our combination of findings of reverse association between vSTM capacity and PT-OC connectivity in aging together with the microstructural alterations of PT-OC tract are in agreement with the PASA theory with respect to the alteration of posterior brain structures. The findings of structural alterations of PT-OC tracts and reduced vSTM capacity is also in agreement with the STAC theory suggesting that neural degradation affects cognitive functions in aging individuals.

Together, these findings suggest that aging modifies the microstructural properties of the tracts connecting posterior thalamus to occipital cortices and thus make those tracts an ideal candidate for mediating the effect of aging on vSTM capacity. This would fit with previous findings on the mediating role of WM integrity in age–behavior relationships (Raz et al., 2005; Burgmans et al., 2011; Brickman et al., 2012; Salami et al., 2012; Samanez-Larkin et al., 2012).

Further studies using magnetization transfer ratio and/or diffusion MRI methods that can resolve intravoxel structure such as high angular resolution diffusion imaging (Tuch et al., 2003) could help yield further information regarding the affected white-matter characteristics.

4.3. Limitations

Our study has several limitations. First, we used a cross-sectional sample. Thus, although we could examine the effect of age on PT-OC structural connectivity with vSTM capacity between individuals, we cannot generalize our findings to intra-individual changes over the lifespan (Salthouse et al., 2011). Moreover, it is difficult to interpret our results in terms of underlying microscopic changes since the number of streamlines generated by probtrackx is not a direct measure of anatomical connectivity and their relationship to the underlying anatomy is rather unclear (Jones, 2010; Jones et al., 2013; Jbabdi and Johansen-Berg, 2011). Several factors can influence the number of streamlines, such as the organization of myelin in regions bordering cortical grey matter (Reveley et al., 2015), fanning fibers and crossing fibers with fewer crossing fibers leading to increased connectivity values (Jbabdi and Johansen-Berg, 2011; Thomas et al., 2014; Reveley et al., 2015; Donahue et al., 2016). Moreover, dense white-matter fiber bundles at the grey-matter/white-matter boundary would hinder the tractography detection of weaker crossing fibers entering or exiting grey matter in sulcal fundi and thus influence the number of streamlines. Crossing fibers are also a limitation of the tensor model and thus will also affect FA, MD, RD and AD values. Finally, in addition to fiber architecture, it has been shown that FA was influenced by axonal degeneration, changes in packing density or demyelination (Takahashi et al., 2002). Nevertheless, without additional analysis at a higher resolution, we cannot disentangle which mechanism underlie a change in diffusivity indices so our use of the word “microstructural changes” should be considered with care. In general, the neuroanatomical study of postmortem tissue at higher resolution or the use of more advanced and specialized biophysical models and sequences such as NODDI, CHARMED or myelin water imaging could help identify which actual mechanisms are responsible.

5. Conclusion

We investigated whether age-related differences exist in the

association between vSTM capacity and the structural connectivity of posterior thalamus to visual cortices. In addition to a reduced vSTM capacity and aberrant PT-OC connection probability, we found that the relationship between vSTM capacity *K* and PT-OC connection probability was significantly modified by age. In young adults, vSTM capacity *K* was significantly negatively associated with PT-OC connection probability, whereas in older adults, this association was positive. Interestingly, we also found reduced fractional anisotropy and increased mean diffusivity in PT-OC tracts with aging, which suggests that the inversion of the association between PT-OC connection probability and vSTM capacity *K* with aging might reflect age-related differences in white-matter properties. Accordingly, we propose that age-related differences in vSTM capacity might be modulated by the microstructure and connectivity of WM between posterior thalamus and occipital cortices.

Acknowledgments

We thank Erika Künstler and Annette Abraham for their help with the recruitment and TVA data collection as well as Tim Reeβ and Gabriel Castrillon for their coding support. We are grateful to the staff of the Department of Neuroradiology in Munich, particularly Dr. Christine Preibisch and Stephan Kaczmarz, for showing us how to operate the scanner. Most importantly, we thank all our study participants for their efforts to take part in this study.

This work was supported by the EU Marie Curie Training Network INDIREA (ITN- 2013–606901 to H.J.M., and K.F.), Deutsche Forschungsgemeinschaft (FI 1424/2-1 to K.F. and SO 1336/1-1 to C.S.), German Federal Ministry of Education and Science (BMBF 01ER0803 to C.S.) and the Kommission für Klinische Forschung, Technische Universität München (KKF 8765162 to C.S).

Appendix A. Supplementary data

Supplementary data to this article can be found online at https://doi.org/10.1016/j.neuroimage.2019.116440.

Author contributions

Aurore Menegaux: Conceptualization, Methodology, Investigation, Software, Validation, Formal analysis, Data curation, Writing Original Draft, Writing Review & Editing, Visualization.

Felix J. B. Bäuerlein: Methodology, Software, Formal analysis, Visualization.

Aliki Vania: Methodology, Formal analysis, Data curation.

Natan Napiorkowski: Resources, Investigation, Formal analysis, Data curation.

Julia Neitzel: Resources, Investigation, Project administration.

Adriana L. Ruiz-Rizzo: Investigation.

Hermann J Müller: Project administration, Funding acquisition, Supervision, Writing Review & Editing.

Christian Sorg: Conceptualization, Project administration, Funding acquisition, Supervision, Writing Review & Editing.

Kathrin Finke: Conceptualization, Project administration, Funding acquisition, Supervision, Writing Review & Editing.

Data and code availability statement

The data are not publicly available, as further consent from the participants of this study would be.

References

Arnold, J.F., Zwiers, M.P., Fitzgerald, D.A., van Eijndhoven, P., Becker, E.S., Rinck, M., Fernandez, G., Speckens, A.E., Tendolkar, I., 2012. Fronto-limbic microstructure and structural connectivity in remission from major depression. Psychiatry Res. 204 (1), 40–48.

Assaf, Y., Blumenfeld-Katzir, T., Yovel, Y., Basser, P.J., 2008. AxCaliber: a method for measuring axon diameter distribution from diffusion MRI. Magn. Reson. Med. 59, 1347–1354.

Baghat, Y.A., Beaulieu, C., 2004. Diffusion anisotropy in subcortical white matter and cortical gray matter: changes with aging and the role of CSF-suppression. J. Magn. Reson. Imaging 20, 216–227.

Barrick, T.R., Charlton, R.A., Clark, C.A., Markus, H.S., 2010. White matter structural decline in normal ageing: a prospective longitudinal study using tract-based spatial statistics. Neuroimage 51, 565–577.

Bartzokis, G., Sultzer, D., Lu, P.H., Nuechterlein, K.H., Mintz, J., Cummings, J.L., 2004. Heterogeneous age-related breakdown of white matter structural integrity: implications for cortical "disconnection" in aging and Alzheimer's disease. Neurobiol. Aging 25, 843–851.

Basser, P.J., 1995. Inferring microstructural features and the physiological state of tissues from diffusion-weighted images. NMR Biomed. 8 (7–8), 333–344.

Beaulieu, C., 2002. The basis of anisotropic water diffusion in the nervous system—a technical review. NMR Biomed. 15 (7–8), 435–455.

Beck, A.T., Steer, R.A., Brown, G.K., 1996. Manual for the Beck Depression Inventory-II, second ed. The Psychological Corporation, San Antonio, TX.

Behrens, T.E., Johansen-Berg, H., Woolrich, M.W., Smith, S.M., Wheeler-Kingshott, C.A., Boulby, P.A., Barker, G.J., Sillery, E.L., Sheehan, K., Ciccarelli, O., Thompson, A.J., Brady, J.M., Matthews, P.M., 2003. Non-invasive mapping of connections between human thalamus and cortex using diffusion imaging. Nat. Neurosci. 6 (7), 750–757.

Behrens, T.E., Berg, H.J., Jbabdi, S., Rushworth, M.F., Woolrich, M.W., 2007. Probabilistic diffusion tractography with multiple fibre orientations: what can we gain? Neuroimage 34 (1), 144–155.

Bennett, I.J., Madden, D.J., Vaidya, C.J., Howard, D.V., Howard, J.H., 2010. Age-related differences in multiple measures of white matter integrity: a diffusion tensor imaging study of healthy aging. Hum. Brain Mapp. 31 (3), 378–390.

Brickman, A.M., Meier, I.B., Korgaonkar, M.S., Provenzano, F.A., Grieve, S.M., Siedlecki, K.L., Wasserman, B.T., Williams, L.M., Zimmerman, M.E., 2012. Testing the white matter retrogenesis hypothesis of cognitive aging. Neurobiol. Aging 33, 1699–1715.

Bundesen, C., 1990. A theory of visual attention. Psychol. Rev. 97, 523–547.

Bundesen, C., Habekost, T., Kyllingsbaek, S., 2005. A neural theory of visual attention: bridging cognition and neurophysiology. Psychol. Rev. 112, 291–328.

Burgmans, S., Gronenschild, E.H., Fandakova, Y., Shing, Y.L., van Boxtel, M.P., Vuurman, E.F., Uylings, H.B., Jolles, J., Raz, N., 2011. Age differences in speed of processing are partially mediated by differences in axonal integrity. Neuroimage 55, 1287–1297.

Burzynska, A.Z., Preuschhof, C., Backman, L., Nyberg, L., Li, S.C., Lindenberger, U., Heekeren, H.R., 2010. Age-related differences in white-matter microstructure: region-specific patterns of diffusivity. Neuroimage 49 (3), 2104–2112.

Chen, T., Naveh-Benjamin, M., 2012. Assessing the associative deficit in older adults in long-term and short-term/working memory. Psychol. Aging 27 (3), 666–682.

Concha, L., Gross, D.W., Wheatley, B.M., Beaulieu, C., 2006. Diffusion tensor imaging of time-dependent axonal and myelin degradation after corpus callosotomy in epilepsy patients. Neuroimage 32, 1090–1099.

Courchesne, E., Chisum, H.J., Townsend, J., Cowles, A., Covington, J., Egaas, B., Harwood, M., Hinds, S., Press, G.A., 2000. Normal brain development and aging: quantitative analysis at in vivo MR imaging in healthy volunteers. Radiology 216 (3), 672–682.

Cowan, N., 2001. The magical number 4 in short-term memory: a reconsideration of mental storage capacity. Behav. Brain Sci. 24, 87–114.

Cowan, N., 2010. Multiple concurrent thoughts: the meaning and developmental neuropsychology of working memory capacity. Dev. Neuropsychol. 35 (5), 447–474.

Davis, S.W., Dennis, N.A., Daselaar, S.M., Fleck, M.S., Cabeza, R., 2008. Que PASA? The posterior-anterior shift in aging. Cerebr. Cortex 18 (5), 1201–1209.

Donahue, C.J., Sotiropoulos, S.N., Jbabdi, S., Hernandez-Fernandez, M., Behrens, T.E., Dyrby, T., Coalson, T., Kennedy, H., Knoblauch, H., Van Essen, D.C., Glasser, M.F., 2016. Using diffusion tractography to predict cortical connection strength and distance: a quantitative comparison with tracers in the monkey. J. Neurosci. 36 (25), 6758–6770.

Duarte, A., Hearons, P., Jiang, Y., Delvin, M.C., Newsome, R.N., Verhaeghen, P., 2013. Retrospective attention enhances visual working memory in the young but not the old: an ERP study. Psychophysiology 505, 465–476.

Dyrholm, M., Kyllingsbaek, S., Espeseth, T., Bundesen, C., 2011. Generalizing parametric models by introducing trial-by-trial parameter variability: the case of TVA. J. Math. Psychol. 55 (6), 416–429.

Fama, R., Sullivan, E.V., 2015. Thalamic structures and associated cognitive functions: relations with age and aging. Neurosci. Biobehav. Rev. 54, 29–37.

Finke, K., Bublak, P., Krummenacher, J., Kyllingsbæk, S., Müller, H.J., Schneider, W.X., 2005. Usability of a theory of visual attention (TVA) for parameter-based measurement of attention I: evidence from normal subjects. J. Int. Neuropsychol. Soc. 11, 832–842.

Finke, K., Bublak, P., Zihl, J., 2006. Visual spatial and visual pattern working memory: neuropsychological evidence for a differential role of left and right dorsal visual brain. Neuropsychologia 44 (4), 649–661.

Folstein, M.F., Folstein, S.E., McHugh, P.R., 1975. "Mini-mental state". A practical method for grading the cognitive state of patients for the clinician. J. Psychiatr. Res. 12 (3), 189–198.

Fukuda, K., Vogel, E.K., Awh, E., Mayr, E., 2010. Quantity not quality: the relationship between fluid intelligence and working memory capacity. Psychon. Bull. Rev. 17, 673–679.

Gazzaley, A., Cooney, J.W., McEvoy, K., Knight, R.T., D'Esposito, M., 2005. Top-down enhancement and suppression of the magnitude and speed of neural activity. J. Cogn. Neurosci. 17 (3), 507–517.
Ge, Y., Grossman, R.I., Babb, J.S., Rabin, M.L., Mannon, L.J., Kolson, D.L., 2002. Age-related total gray matter and white matter changes in normal adult brain. Part I: volumetric MR imaging analysis. AJNR Am. J. Neuroradiol. 23 (8), 1327–1333.
Habekost, T., Rostrup, E., 2007. Visual attention capacity after right hemisphere lesions. Neuropsychologia 45, 1474–1488.
Habekost, T., Starrfelt, R., 2009. Visual attention capacity: a review of TVA-based patients studies. Scand. J. Psychol. 50 (1), 23–32.
Hebb, D.O., 1949. Organization of Behavior. Wiley, New York.
Herting, M.M., Colby, J.B., Sowell, E.R., Nagel, B.J., 2013. White matter connectivity and aerobic fitness in male adolescents. Dev. Cogn. Neurosci. 7, 65–75. https://doi.org/10.1016/j.dcn.2013.11.003.
Hugenschmidt, C.E., Peiffer, A.M., Kraft, R.A., Casanova, R., Deibler, A.R., Burdette, J.H., Maldjian, J.A., Laurienti, P.J., 2008. Relating imaging indices of white matter integrity and volume in healthy older adults. Cerebr. Cortex 18, 433–442.
Hughes, E.J., Bond, J., Svrckova, P., Makropoulos, A., Ball, G., Sharp, D.J., Edwards, A.D., Hajnal, J.V., Counsell, S.J., 2012. Regional changes in thalamic shape and volume with increasing age. Neuroimage 63, 1134–1142.
Huster, R.J., Westerhausen, R., Kreuder, F., Schweiger, I., Wittling, W., 2009. Hemispheric and gender related differences in the midcingulum bundle: a DTI study. Hum. Brain Mapp. 30, 383–391.
Jbabdi, S., Johansen-Berg, H., 2011. Tractography: where do we go from here? Brain Connect. 1 (3), 169–183.
Jbabdi, S., Sotiropoulos, S.N., Haber, S.N., Van Essen, D.C., Behrens, T.E., 2015. Measuring macroscopic brain connections in vivo. Nat. Neurosci. 18 (11), 1546–1555.
Jenkinson, M., Beckmann, C.F., Behrens, T.E., Woolrich, M.W., Smith, S.M., 2012. FSL. Neuroimage 62 (2), 782–790.
Johnson, M.K., MacMahon, R.P., Robinson, B.M., Harvey, A.,N., Hahn, B., Leonard, C.J., Luck, S.J., Gold, J.M., 2013. The relationship between working memory capacity and broad measures of cognitive ability in healthy adults and people with schizophrenia. Neuropsychology 27, 220–229.
Johnson, R.T., Yeatman, J.D., Wandell, B.A., Buonocore, M.H., Amaral, D.G., Nordahl, C.W., 2014. Diffusion properties of major white matter tracts in young, typically developing children. Neuroimage 88, 143–154.
Jones, D.K., 2010. Challenges and limitations of quantifying connectivity in the human brain in vivo with diffusion MRI. Imaging Med. 2, 341–355.
Jones, D.K., Knosche, T.R., Turner, R., 2013. White matter integrity, fiber count, and other fallacies: the do's and don'ts of diffusion MRI. Neuroimage 73, 239–254.
Jost, K., Bryck, R.L., Vogel, E.K., Mayr, U., 2011. Are old adults just like low working memory young adults? Filtering efficiency and age differences in visual working memory. Cerebr. Cortex 21, 1147–1154.
Khalsa, S., Mayhew, S.D., Chechlacz, M., Bagary, M., Bagshaw, A.P., 2014. The structural and functional connectivity of the posterior cingulate cortex: comparison between deterministic and probabilistic tractography for the investigation of structure-function relationships. Neuroimage 102 (Pt 1), 118–127. https://doi.org/10.1016/j.neuroimage.2013.12.022.
Kumar, R., Chavez, A.S., Macey, P.M., Woo, M.A., Harper, R.M., 2013. Brain axial and radial diffusivity changes with age and gender in healthy adults. Brain Res. 1512, 22–36.
Lasiene, J., Shupe, L., Perlmutter, S., Horner, P., 2008. No evidence for chronic demyelination in spared axons after spinal cord injury in a mouse. J. Neurosci. 28 (15), 3887–3896. https://doi.org/10.1523/JNEUROSCI.4756-07.2008.
Lebel, C., Walker, L., Leemans, A., Phillips, L., Beaulieu, C., 2008. Microstructural maturation of the human brain from childhood to adulthood. Neuroimage 40 (3), 1044–1055.
Luck, S.J., Vogel, E.K., 1997. The capacity of visual working memory for features and conjunctions. Nature 390, 279–281.
Luck, S.J., Vogel, E.K., 2013. Visual working memory capacity: from psychophysics and neurobiology to individual differences. Trends Cogn. Sci. 17 (8), 391–400. https://doi.org/10.1016/j.tics.2013.06.006.
Malloy, P., Correia, S., Stebbins, G., Laidlaw, D.H., 2007. Neuroimaging of white matter in aging and dementia. Clin. Neuropsychol. 21 (1), 73–109.
Malone, I.B., Leung, K.K., Clegg, S., Barnes, J., Whitwell, J.L., Ashburner, J., Fox, N.C., Ridgway, G.R., 2015. Accurate automatic estimation of total intracranial volume: a nuisance variable with less nuisance. Neuroimage 104, 366–372.
Marner, L., Nyengaard, J.R., Tang, Y., Pakkenberg, B., 2003. Marked loss of myelinated nerve fibers in the human brain with age. J. Comp. Neurol. 462 (2), 144–152.
McAvinue, L.P., Habekost, T., Johnson, K.A., Kyllingsbaek, S., Vangkilde, S., Bundesen, C., Robertson, I.H., 2012. Sustained attention, attentional selectivity, and attentional capacity across the lifespan. Atten. Percept. Psychophys. 74 (8), 1570–1582.
Meier-Ruge, W., Ulrich, J., Bruhlmann, M., Meier, E., 1992. Age-related white matter atrophy in the human brain. Ann. N. Y. Acad. Sci. 673, 260–269.
Menegaux, A., Meng, C., Neitzel, J., Bauml, J.G., Muller, H.J., Bartmann, P., Wolke, D., Wohlschläger, A.M., 2017. Impaired visual short-term memory capacity is distinctively associated with structural connectivity of the posterior thalamic radiation and the splenium of the corpus callosum in preterm-born adults. Neuroimage 150, 68–76.
Menegaux, A., Napiorkowski, N., Neitzel, J., Ruiz-Rizzo, A.L., Petersen, A., Müller, H.J., Sorg, C., Finke, K., 2019. Theory of visual attention's thalamic model for visual short-term memory capacity and top-down control: evidence from a thalamo-cortical structural connectivity analysis. Neuroimage 195, 67–77.
Meng, C., Bäuml, J.G., Daamen, M., Jaekel, J., Neitzel, J., Scheef, L., Busch, B., Baumann, N., Boecker, H., Zimmer, C., Bartmann, P., Wolke, D., Wohlschläger, A.M., Sorg, C., 2015. Extensive and interrelated subcortical white and gray matter alterations in preterm-born adults. Brain Struct. Funct. 221 (4), 2109–2121.
Minati, L., Grisoli, M., Buzzone, M.G., 2007. MR spectroscopy, functional MRI, and diffusion-tensor imaging in the aging brain: a conceptual review. J. Geriatr. Psychiatry Neurol. 20, 3–21.
Monge, Z.A., Madden, D.J., 2016. Linking cognitive and visual perceptual decline in healthy aging: the information degradation hypothesis. Neurosci. Biobehav. Rev. 69, 166–173. https://doi.org/10.1016/j.
Naveh-Benjamin, M., 2000. Adult age differences in memory performance: tests of an associative deficit hypothesis. J. Exp. Psychol. Learn. Mem. Cogn. 26 (5), 1170–1187.
Noack, H., Lövdén, M., Lindenberger, U., 2012. Normal aging increases discriminal dispersion in visuospatial short-term memory. Psychol. Aging 27 (3), 627–637. https://doi.org/10.1037/a0027251.
Nyberg, L., Lövdén, M., Riklund, K., Lindenberger, U., Bäckman, L., 2012. Memory aging and brain maintenance. Trends Cogn. Sci. 16 (5), 292–305. https://doi.org/10.1016/j.tics.2012.04.005.
O'Sullivan, M., Jones, D.K., Summers, P.E., Morris, R.G., Williams, S.C., Markus, H.S., 2001. Evidence for cortical "disconnection" as a mechanism of age-related cognitive decline. Neurology 57, 632–638.
Oldfield, R.C., 1971. The assessment and analysis of handedness: the Edinburgh inventory. Neuropsychologia 9 (1), 97–113.
Park, D.C., Reuter-Lorenz, P., 2009. The adaptive brain: aging and neurocognitive scaffolding. Annu. Rev. Psychol. 60, 173–196. https://doi.org/10.1146/annurev.psych.59.103006.093656.
Peich, M.-C., Husain, M., Bays, P.M., 2013. Age-related decline of precision and binding in visual working memory. Psychol. Aging 28 (3), 729–743.
Pertzov, Y., Heider, M., Liang, Y., Husain, M., 2015. Effects of healthy ageing on precision and binding of object location in visual short term memory. Psychol. Aging 30 (1), 26–35. https://doi.org/10.1037/a0038396.
Peters, A., Sethares, C., Killiany, R.J., 2001. Effects of age on the thickness of myelin sheaths in monkey primary visual cortex. J. Comp. Neurol. 435 (2), 241–248.
Peters, A., 2002. The effects of normal aging on myelin and nerve fibers: a review. J. Neurocytol. 31, 581–593.
Peters, A., 2009. The effects of normal aging on myelinated nerve fibers in monkey central nervous system. Front. Neuroanat. 3, 11. https://doi.org/10.3389/neuro.05.011.2009.
Pfefferbaum, A., Sullivan, E.V., Hedehus, M., Lim, K.O., Adalsteinsson, E., Moseley, M., 2000. Age-related decline in brain white matter anisotropy measured with spatially corrected echo-planar diffusion tensor imaging. Magn. Reson. Med. 44, 259–268.
Pierpaoli, C., Basser, P.J., 1996. Toward a quantitative assessment of diffusion anisotropy. Magn. Reson. Med. 36 (6), 893–906.
Pierpaoli, C., Jezzard, P., Basser, P.J., Barnett, A., Di Chiro, G., 1996. Diffusion tensor MR imaging of the human brain. Radiology 201, 637–648.
Raz, N., Lindenberger, U., Rodrigue, K.M., Kennedy, K.M., Head, D., Williamson, A., Dahle, C., Gerstorf, D., Acker, J.D., 2005. Regional brain changes in aging healthy adults: general trends, individual differences and modifiers. Cerebr. Cortex 15, 1676–1689.
Raz, N., Rodrigue, K.M., 2006. Differential aging of the brain: patterns, cognitive correlates and modifiers. Neurosci. Biobehav. Rev. 30 (6), 730–734.
Reuter-Lorenz, P.A., Park, D.C., 2014. How does it STAC up? Revisiting the scaffolding theory of aging and cognition. Neuropsychol. Rev. 24 (3), 355–370. https://doi.org/10.1007/s11065-014-9270-9.
Reveley, C., Seth, A.K., Pierpaoli, C., Silva, A.C., Yu, D., Saunders, R.C., Leopold, D.A., Ye, F.Q., 2015. Superficial white matter fiber systems impede detection of long-range cortical connections in diffusion MR tractography. Proc. Natl. Acad. Sci. U. S. A. 112, 2820–2828.
Rilling, J.K., Glasser, M.F., Preuss, T.M., 2008. The evolution of the arcuate fasciculus revealed with comparative DTI. Nat. Neurosci. 11 (4), 426–428.
Rorden, C., Karnath, H.O., Bonilha, L., 2007. Improving lesion-symptom mapping. J. Cog. Neurosci. 19 (7), 1081–1088.
Salami, A., Eriksson, J., Nilsson, L.G., Nyberg, L., 2012. Age-related white matter microstructural differences partly mediate age-related decline in processing speed but not cognition. Biochim. Biophys. Acta 408–415, 1822.
Salat, D.H., Kaye, J.A., Janowsky, J.S., 1999. Prefrontal gray and white matter volumes in healthy aging and Alzheimer disease. Arch. Neurol. 56 (3), 338–344.
Salat, D.H., Chen, J.J., Van der Kouwe, A.J., Greve, D.N., Fischl, B., Rosas, H.D., 2011. Hippocampal degeneration is associated with temporal and limbic gray matter/white matter tissue contrast in Alzheimer's disease. Neuroimage 54 (3), 1795–1802.
Salthouse, T.A., 1994. The nature of the influence of speed on adult age differences in cognition. Dev. Psychol. 30 (2), 240–259.
Salthouse, T.,A., 1996. The processing-speed theory of adult age differences in cognition. Psychol. Rev. 103 (3), 403–428.
Salthouse, T.A., 2011. Effects of age on time-dependent cognitive change. Psychol. Sci. 22 (5), 682–688.
Samanez-Larkin, G.R., Levens, S.M., Perry, L.M., Dougherty, R.F., Knutson, B., 2012. Frontostriatal white matter integrity mediates adult age differences in probabilistic reward learning. J. Neurosci. 32, 5333–5337.
Sander, M.C., Werkle-Bergner, M., Lindenberger, U., 2011. Contralateral delay activity reveals life-span age differences in top-down modulation of working memory contents. Cerebr. Cortex 12, 2809–2819.
Schneider, B.,A., Pichora-Fuller, M.,K., 2000. Implications of perceptual deterioration for cognitive aging research. In: Craik, F.I.M., Salthouse, T.A. (Eds.), The Handbook of Aging and Cognition. Lawrence Erlbaum Associates Publishers, pp. 155–219.

Silver, N.C., Barker, G.J., MacManus, D.G., Tofts, P.S., Miller, D.H., 1997. Magnetisation transfer ratio of normal brain white matter: a normative database spanning four decades of life. J. Neurol. Neurosurg. Psychiatry 62, 223–228.
Smith, E.E., Jonides, J., Koeppe, R.A., Awh, E., 1995. Spatial versus object working memory: PET investigations. J. Cogn. Neurosci. 7, 337–358.
Smith, S., Jenkinson, M., Woolrich, M., Beckmann, C., Behrens, T., Johansen-Berg, H., Bannister, P., DeLuca, M., Drobnjak, I., Flitney, D., Niazy, R., Saunders, J., Vickers, J., Zhang, Y., DeStefano, N., Brady, J., Matthews, P., 2004. Advances in functional and structural MRimage analysis and implementation as FSL. Neuroimage 23 (S1), 208–219.
Sperling, G., 1960. The information available in brief visual presentations. Psychol. Monogr. (Gen. Appl.) 74, 1.
Sullivan, E.V., Rohlfing, T., Pfefferbaum, A., 2010a. Quantitative fiber tracking of lateral and interhemispheric white matter systems in normal aging: relations to timed performance. Neurobiol. Aging 31 (3), 464–481.
Sullivan, E.V., Zahr, N.M., Rohlfing, T., Pfefferbaum, A., 2010b. Fiber tracking functionally distinct components of the internal capsule. Neuropsychologia 48 (14), 4155–4163.
Takahashi, M., Hackney, D.B., Zhang, G., Wehrli, S.L., Wright, A.C., O'Brien, W.T., Uematsu, H., Wehrli, S.W., Selzer, M.E., 2002. Magnetir resonance microimaging of intraaxonal water diffusion in live excised lamprey in spinal cord. Proc. Nat. Acad. Sci. U.S.A. 99, 16192–16196.
Teipel, S.J., Meindl, T., Wagner, M., Stieltjes, B., Reuter, S., Hauenstein, K.H., Filippi, M., Ernemann, U., Reiser, M.F., Hampel, H., 2010. Longitudinal changes in fiber tract integrity in healthy aging and mild cognitive impairment: a DTI follow-up study. J. Alzheimer's Dis. 22, 507–522.
Thomas, C., Ye, F.Q., Irfanoglu, M.O., Modi, P., Saleem, K.S., Leopold, D.A., Pierpaoli, C., 2014. Anatomical accuracy of brain connections derived from diffusion MRI tractography is inherently limited. Proc. Natl. Acad. Sci. U. S. A. 111, 16574–16579.
Todd, J.J., Marois, R., 2005. Posterior parietal cortex activity predicts individual differences in visual short-term memory capacity. Cognit. Affect Behav. Neurosci. 5 (2), 144–155.
Tuch, D.S., Reese, T.G., Wiegell, M.R., Wedeen, V.J., 2003. Diffusion MRI of complex neural architecture. Neuron 40, 885–895.
Verhaegen, P., Marcoen, A., Goossens, L., 1993. Facts and fiction about memory aging: a quantitative integration of research findings. J. Gerontol.: Psychol. Sci. 48, 157–171.
Vernooij, M.W., de Groot, M., van der Lugt, A., Ikram, M.A., Krestin, G.P., Hofman, A., Niessen, W.J., Breteler, M.M., 2008. White matter atrophy and lesion formation explain the loss of structural integrity of white matter in aging. Neuroimage 43 (3), 470–477.
Vogel, E.K., Machizawa, M.G., 2004. Neural activity predicts individual differences in visual working memory capacity. Nature 428, 748–751.
Walhovd, K.B., Westlye, L.T., Amlien, I., Espeseth, T., Reinvang, I., Raz, N., Agartz, I., Salat, D.H., Greve, D.N., Fischl, B., Dale, A.M., Fjell, A.M., 2011. Consistent neuroanatomical age-related volume differences across multiple samples. Neurobiol. Aging 32 (5), 916–932.
Wang, Y., Zhou, T., Ma, Y., Leventhal, A.,G., 2005. Degradation of signal timing in cortical area V1 and V2 of senescent monkeys. Cerebr. Cortex 15, 403–408.
Westlye, L.T., Walhovd, K.B., Dale, A.M., Bjørnerud, A., Due-Tønnessen, P., Engvig, A., Grydeland, H., Tamnes, C.K., Østby, Y., Fjell, A.M., 2010. Life-span changes of the human brain white matter: diffusion tensor imaging (DTI) and volumetry. Cerebr. Cortex 20 (9), 2055–2068.
Wiegand, I., Töllner, T., Dyrholm, M., Müller, H.J., Bundesen, C., Finke, K., 2014a. Neural correlates of age-related decline and compensation in visual attention capacity. Neurobiol. Aging 35, 2161–2173.
Wiegand, I., Töllner, T., Habekost, T., Dyrholm, M., Müller, H.J., Finke, K., 2014b. Distinct neural markers of TVA-based visual processing speed and short-term storage capacity parameters. Cerebr. Cortex 24, 1967–1978.
Wiegand, I., Lauritzen, M.J., Osler, M., Mortensen, E.L., Rostrup, E., Rask, L., Richard, N., Horwitz, A., Benedek, K., Vangkilde, S., Petersen, A., 2018. EEG correlates of visual short-term memory in older age vary with adult lifespan cognitive development. Neurobiol. Aging 62, 210–220.
Wozniak, J.R., Lim, K.O., 2006. Advances in white matter imaging: a review of in vivo magnetic resonance methodologies and their applicability to the study of development and aging. Neurosci. Biobehav. Rev. 30 (6), 762–774, 2006.
Zahr, N.M., Rohlfing, T., Pfefferbaum, A., Sullivan, E.V., 2009. Problem solving, working memory, and motor correlates of association and commissural fiber bundles in normal aging: a quantitative fiber tracking study. Neuroimage 44, 1050–1062.
Zhang, Y., Du, A.T., Hayasaka, S., Jahng, G.H., Hlavin, J., Zhan, W., Weiner, M.W., Schuff, N., 2010a. Patterns of age-related water diffusion changes in human brain by concordance and discordance analysis. Neurobiol. Aging 31 (11), 1991–2001.
Zhang, D., Snyder, A.Z., Shimony, J.S., Fox, M.D., Raichle, M.E., 2010b. Noninvasive functional and structural connectivity mapping of the human thalamocortical system. Cerebr. Cortex 20 (5), 1187–1194.